Physics of Semiconductors.
Physics of Low-Dimensional Structures
and Nanostructures

UDC 536.42+539.19

https://www.doi.org/10.33910/2687-153X-2022-3-1-43-50

Dielectric spectroscopy of VO_2 nanocrystalline films

R. A. Castro Arata✉[1], A. V. Ilinskiy[2], V. A. Klimov[2], M. E. Pashkevish[3], E. B. Shadrin[2]

[1] Herzen State Pedagogical University of Russia, 48 Moika Emb., Saint Petersburg 191186, Russia
[2] Ioffe Institute, 26 Politekhnicheskaya Str., Saint Petersburg 194021, Russia
[3] Peter the Great St. Petersburg Polytechnic University,
29 Politekhnicheskaya Str., Saint Petersburg 195251, Russia

Authors

Rene Alejandro Castro Arata, ORCID: 0000-0002-1902-5801, e-mail: recastro@mail.ru

Aleksandr V. Ilinskiy, e-mail: Ilinskiy@mail.ioffe.ru

Vladimir A. Klimov, ORCID: 0000-0002-9096-7594, e-mail: vlad.a.klimov@mail.ioffe.ru

Marina E. Pashkevish, ORCID: 0000-0002-3373-4129, e-mail: marpash@yandex.ru

Evgeniy B. Shadrin, ORCID: 0000-0002-1423-2852, e-mail: shadr.solid@mail.ioffe.ru

For citation: Castro Arata, R. A., Ilinskiy, A. V., Klimov, V. A., Pashkevish, M. E., Shadrin, E. B. (2022) Dielectric spectroscopy of VO_2 nanocrystalline films. *Physics of Complex Systems*, 3 (1), 43–50. https://www.doi.org/10.33910/2687-153X-2022-3-1-43-50

Received 20 December 2021; reviewed 12 January 2022; accepted 12 January 2022.

Funding: The reported study was funded by Russian Foundation for Basic Research (RFBR), Project No. 20-07-00730.

Abstract. The article describes the first reported case of applying dielectric spectroscopy to study nontrivial details of size dependences of phase transformation parameters in nanocrystallites of VO_2 films. The method allows to identify the electrophysical parameters of nanocrystalline sets of different sizes and random location on the VO_2 substrate. The article investigates the martensitic nature of the Mott-Peierls semiconductor-metal phase transition in crystalline VO_2 films.

Keywords: dielectric spectroscopy, vanadium dioxide films, VO_2, semiconductor-metal phase transition, correlation effects

Introduction

When studying the parameters of the electrical response of a material (Prokhorov 1994), dielectric spectroscopy pays special attention to the tangent of the dielectric loss angle δ—tanδ. For an ideal dielectric between the capacitor plates, the bias current outstrips the hesitation phase of the applied alternating voltage by an angle $\psi = \pi/2$. For a non-ideal dielectric, this angle is smaller according to the law $\delta + \psi = \pi/2$. The smaller the angle δ, the less energy is lost for heat generation. This is essential for the production of large high-quality capacitors. Data on frequency dependence of *tg(f)* is instrumental in the design of insulators for high-voltage power lines as well as for many other practical applications.

The development of highly sensitive dielectric spectrometers with high-speed computers has led to the emergence of dielectric spectroscopy as a method of scientific research.

The aim of our article was to explore semiconductor-metal phase transition (SMPT) in nanocrystalline VO_2 films using dielectric spectroscopy. These films undergo SMPT with an increase of temperature near $T = 340$ K. This transition has a combined nature (Ilinskiy et al. 2012; Shadrin, Il'inskiy 2000) which is of interest from both applied and fundamental points of view.

Experimental technique

The samples studied by dielectric spectroscopy included vanadium dioxide thin films (100 nm) synthesized on insulating glass substrates with a thickness of d = 1 *mm*. The samples were placed in the measuring cell of a dielectric spectrometer shaped as a cylinder with two flat metal electrodes. The cell capacity without a sample was $C_0 = \varepsilon_0 S/d$, where S is the area of mutual overlap of the electrodes and ε_0 is the dielectric constant. A sinusoidal electric voltage U_0 of frequency f was applied to the electrodes. In this case, an alternating current I_0 of the same frequency flowed through the sample, but with a phase shift ψ with respect to the phase of the applied voltage oscillations. Dielectric spectroscopy was applied to measure the following parameters: the amplitude U_o of the applied voltage, the frequency dependences of the amplitude of the current $I_o(f)$ flowing through the sample, and the frequency dependences of the phase difference $\psi(f)$. The spectrometer cell with the sample is a flat capacitor. This means that the computer built into the spectrometer can obtain the following characteristics of dielectric spectra based on the measured values *Uo, Io(f),* and $\psi(f)$:

1) the frequency dependence of the tangent of the dielectric loss angle $tan\delta(f)$ $(\delta = \pi/2-\psi)$ and the frequency dependence of the current amplitude $I_o(f)$;

2) frequency dependences of the real z' and imaginary z'' parts of the total impedance of the sample;

3) frequency dependences of the real ε' and imaginary ε'' parts of the dielectric constant of the sample;

4) frequency dependence of $tan(f)$ together with Cole-Cole diagram $\varepsilon''(\varepsilon')$.

Experimental results

As an initial result, the article presents data on the morphology of the studied film. Fig. 1 shows the atomic-force image of an undoped VO_2 film, and Fig. 2 shows a histogram of the size distribution of film nanocrystallites. It should be noted that the study found two types of nanocrystallites significantly different in their average size. They can be called "large" and "small".

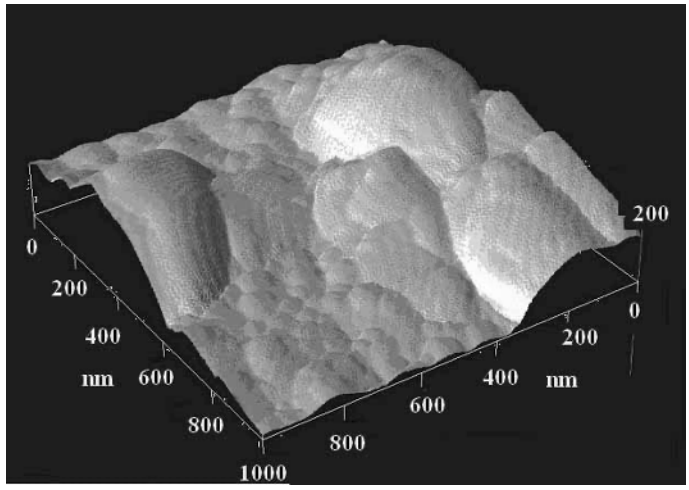

Fig. 1. Atomic force image of the surface of a vanadium dioxide film

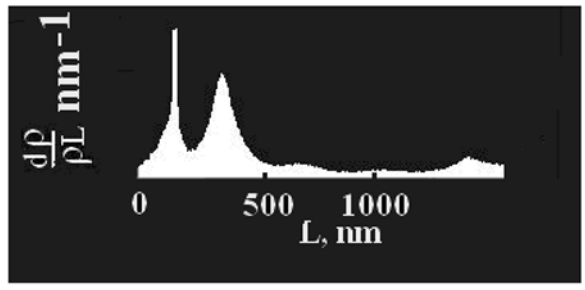

Fig. 2. Size distribution histogram of nanocrystallites

https://www.doi.org/10.33910/2687-153X-2022-3-1-43-50

In what follows we discuss:
1) frequency dependence of *tanδ(f);*
2) Cole-Cole diagram *ε"(ε').*

These results were obtained at different temperatures. As practice shows, these data most effectively reflect both frequency and thermal parameters of the sample (Fig. 3).

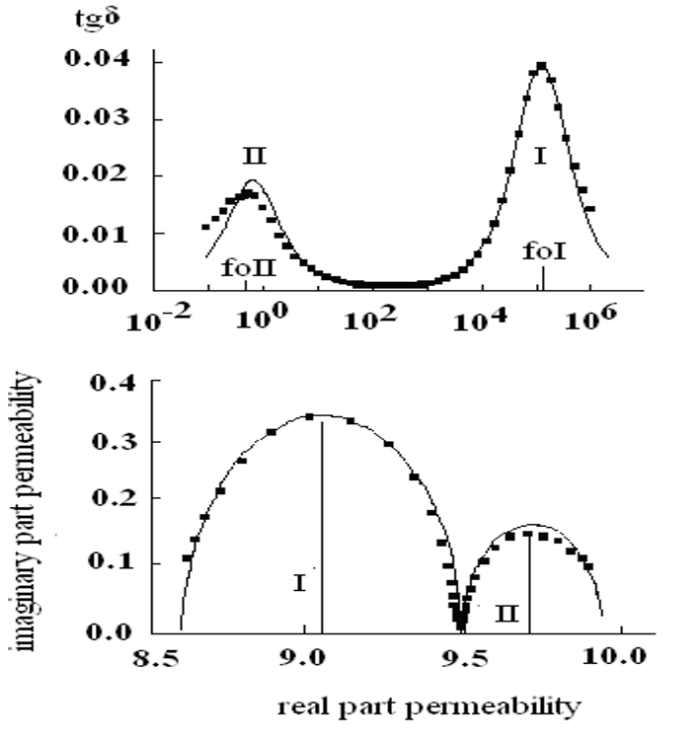

Fig. 3. Frequency dependences of the tangent of the dielectric loss angle *tanδ(f)* and Cole-Cole diagram for a VO_2 film at a temperature of T = 303 K. Dots are the result of the experiment, solid lines are the result of the calculation (C_b = 6.2 pF, *CI* = 33 pF, *RI* = 56.8 kΩ, *Cm* =7.5 pF, *CII*=127 pF, R_{II} = 2.8 GΩ, *C0* = 1.4 pF)

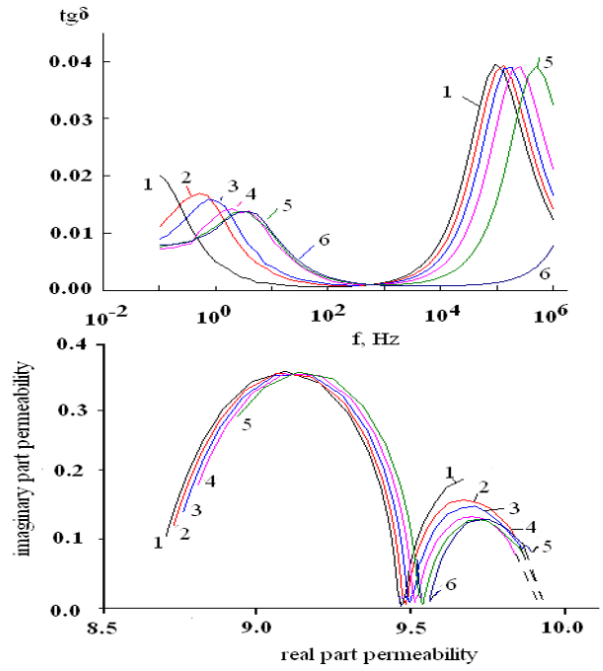

Fig. 4. Frequency dependences of the tangent of the dielectric loss angle *tanδ(f)* and Cole-Cole diagrams for an undoped VO_2 film at different temperatures (experiment): 1–293 K, 2–303 K, 3–313 K, 4–323 K, 5–333 K, 6–343 K

Fig. 3 provides experimental data for the sample temperature T = 303 K. Dots are the result of the experiment, solid lines are the result of the calculation. It is interesting that two maxima of the function *tanδ(f)* are observed at frequencies f_{0I} = 50 kHz and f_{0II} = 1 Hz. The Cole-Cole diagram has two semicircles: a high-frequency semicircle of a large diameter and a low-frequency semicircle of a smaller diameter.

Fig. 4 shows the experimental data for *tanδ(f)* and *ε"(ε')* in the range 293–343 K. With an increase in temperature, the maxima shift unevenly towards high frequencies. The high-frequency maximum in the range 293–323 K shifts to high frequencies by a smaller interval than in the range 323–343 K. The low-frequency maximum shifts in the range T = 293–323 K by a larger frequency interval than in the range T = 323–343 K. The Cole-Cole diagram does not change with temperature.

Mathematical modeling

Dielectric spectroscopy makes it possible to experimentally determine the frequency dependences (dielectric spectra) *tanδ(f)*, *ε'(f)* and *ε"(f)*, that is, construct *ε"(ε')* regardless of the equivalent electrical circuit of the sample. The theory makes it possible to simulate the electrical response of a sample and find analytical expressions that correlate the values *tanδ*, *ε'* and *ε"* with specific parameters of the samples. By comparing the experimental spectra with the calculated ones, the validity of the application of a particular scheme is tested and the numerical values of the parameters of the equivalent circuit model are determined.

In our case, there are two maxima of the function *tgδ(f)* and two semicircles on the Cole-Cole diagram. Therefore, the approach shown in Fig. 5, may be applied in modelling.

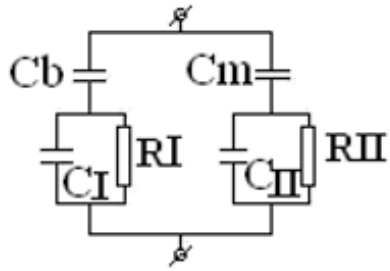

Fig. 5. Equivalent schema

The use of this approach is also justified by the structure of the sample. It takes into account the presence of two sets of film nanocrystallites with very different parameters. These sets are randomly mixed with each other on an insulating substrate. Capacities C_b and C_m are the total capacities of those parts of the substrate on which large and small nanocrystallites are synthesized. Capacities C_I, C_{II} represent the electrical capacities of the sets of nanocrystallites themselves. Electric resistances R_I and R_{II} are connected in parallel to these capacitors in the equivalent circuit, which characterise the through-current flow through the sample.

Mathematical modeling is as follows. The symbolic method of calculation is used to obtain formulas for the frequency dependence of the tangent of the dielectric loss angle, that is, the function *tanδ(f)*. After these we obtain formulas for the frequency dependences of *ε"(ω)* and *ε'(ω)* of the sample ($f = 2\pi\omega$) (Ilinskiy et al. 2020).

$$tg\delta(f) = -(DW + FV) / (FW - DV), \quad (1)$$

$$\varepsilon'(\omega) = (FW - DV)(W^2 + V^2) / \omega C_o[(DW + FV)^2 + (FW - DW)^2], \quad (2)$$

$$\varepsilon''(\omega) = (DW + FV)(W^2 + V^2) / \omega Co[(DW + FV)^2 + (FW - DV)^2], \quad (3)$$

where

$$D = AGM - BGN - BMH - ANH$$
$$F = AGN + AMH + BGM - BHN$$

 https://www.doi.org/10.33910/2687-153X-2022-3-1-43-50

$$W = MG - NH + AG - BH + AM - BN$$
$$V = NG + MH + BG + AH + BM + AN,$$

where

$$A = R_I/(\omega^2 R_I^2 C_I^2 + 1)$$
$$B = -[\omega^2 R_I^2 C_I (C_I + C_b) + 1]/(\omega^3 R_I^2 C_I^2 C_b + \omega C_b)$$
$$M = R_{II}/(\omega^2 R_{II}^2 C_{II}^2 + 1)$$
$$N = -[\omega^2 R_{II}^2 C_{II} (C_{II} + C_m) + 1]/(\omega^3 R_{II}^2 C_{II}^2 C_m + \omega C_m)$$

Expression (1) gives two maxima on the graph of the frequency dependence *tanδ(f),* and expressions (2), (3) — two semicircles on the Cole-Cole — diagram (solid curves in Fig. 3). By varying the values of C_I, C_b, R_I, C_{II}, C_m, R_{II} in accordance with the algorithm (Castro et al. 2021), the best agreement of the experimental data with the calculated data is obtained. The result of the fitting determines the sought values C_I, C_b, R_I, C_{II}, C_m, R_{II} (specific numerical values for the VO_2 film sample are given in the caption to Fig. 3).

Calculations show that as Cole-Cole diagrams do not depend on temperature (Fig. 4), it follows that the temperature shift of both maxima *tanδ(f)* is determined only by the values R_I and R_{II} and the expressions for Cole-Cole diagrams include only the electrical capacities of the sets of grains. Therefore, Fig. 6 shows the calculated temperature dependences of the conductivities $1/R_I\,(T)$ and $1/R_{II}\,(T)$ for two sets of film grains.

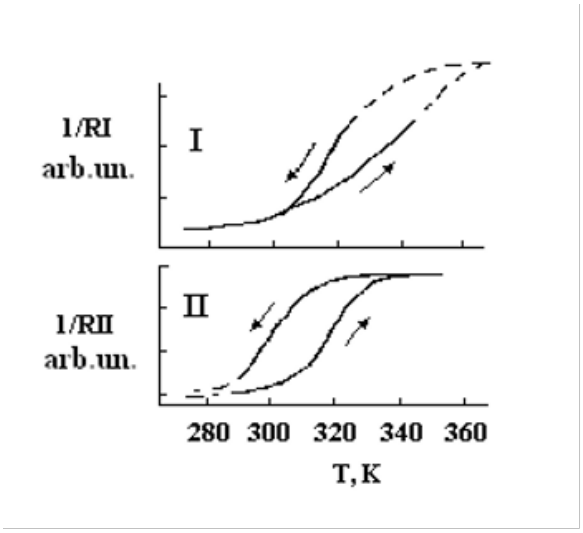

Fig. 6. Thermal hysteresis loops of the electrical conductivity of two sets of grains of the VO_2 film

Figure 6. shows that with an increase in *T*, the numerical values of *R* decrease. Functions $1/R_I(T)$ and $1/R_{II}(T)$ represent the ascending and descending branches of the temperature hysteresis loops of the conductivity of nanocrystallites. The presence of loops indicates semiconductor-metal phase transitions with different values of physical parameters in both sets of VO_2 nanocrystallites. We point out that the set of nanocrystallites, designated by the index I, is characterized by an average resistance R_I = 56 kΩ, and the elements of this set undergo the Peierls structural SMPT at an average temperature of T_{cI} = 340 K. The elements of the set of nanocrystallites, designated by the index II, are characterized by an average resistance $R_{II} = 10^6$ Ω, and the elements of this set perform the Peierls structural SMPT at an average temperature of T_{cII} = 320 K. This indicates a difference in the physical properties of elements in type I and type II sets.

Discussion

Function *tan(f)* has two maxima (f_{0II} = *1 Hz* and f_{0I} = *0.5 MHz*) and the Cole-Cole diagram has two semicircles. This means that the VO_2 film contains two types of relaxators (II and I). One type is characterised by a time constant of 1 *s*, and the other type is characterised by a time constant of 10^{-5} *s*.

These types of relaxators correspond to the two sets of nanocrystallites with significantly different electrophysical properties. In addition, the critical temperatures T_c of the Mott-Peierls SMPT are different for the elements of both sets.

For the low-frequency maximum, the SMPT temperature T_{cII} = 320 K is lower than the transition temperature T_{cI} = 340 K for the high-frequency maximum. This means that in a set of type II, the correlation effects narrow down the E_g of VO_2 nanocrystallites (lower T_c of SMPT) much more than in a set of type I (Castro et al. 2021). It also turned out that the width of the hysteresis loop (20 K) for the low-frequency maximum is almost twice the width of the hysteresis loop (11 K) of the high-frequency maximum. According to the martensitic model of the combined Mott–Peierls SMPT in VO_2 (Il'inskiy et al. 2017), this indicates the presence in the VO_2 film of two sets of nanocrystallites significantly different in their diameter.

Low frequency maximum II of function *tan(f)* corresponds to nanocrystallites with a "small" diameter (wide hysteresis loop), while the high-frequency maximum I corresponds to nanocrystallites with a "large" diameter (narrow hysteresis loop). The presence of two types of nanocrystallites is also evidenced by the histogram of the size distribution of nanocrystallites (Fig. 1).

Thus, the numerical values of C_{II} and R_{II} represent the electrical capacitance and charging resistance of the entire set of "small" nanocrystallites of the film. This causes an electrical response of the film sample at a low frequency $f_{0II} = (2^{1/2}) / R_{II}C_{II}$. The numerical values of C_I and R_I correspond to a set of "large" film nanocrystallites at a high frequency $f_{0I} = (2^{1/2})/R_IC_I$.

We emphasize that the proposed algorithm used to compare the experimental results with the calculated parameters of the equivalent circuit makes it possible to obtain the numerical value of the ratio of the substrate areas S occupied by the two described sets of nanocrystallites. This ratio for the sample under study is $S_{smal;}/S_{large}$ = 1.2. This result can be obtained because our method allows us to separately determine the capacitances of the substrate $C_m = 7.5\ pF$ and $C_b = 6.2\ pF$ from the analysis of the parameters of the Cole-Cole diagram.

The nature of SMPT is difficult to analyze because near T_c vanadium dioxide undergoes two types of SMPT: the Peierls structural transition and the Mott electronic transition (Ilinskiy et al. 2012; Shadrin, Il'inskii 2000). This significantly complicates the simple SMPT model as it is necessary to take into account many-electron interactions. This issue is discussed in detail in our earlier paper (Il'inskiy et al. 2017), therefore, here we present only those excerpts that are important for understanding the proposed statements.

So, at a temperature $T < T_c$ = 340 K vanadium dioxide is a semiconductor, not a metal. This circumstance compels us to assume (on the basis of the considerations described in our earlier papers) that as the temperature decreases to $T < T_c$, neighboring vanadium atoms approach each other in pairs, combining their free electrons on the d_{x2-y2} orbitals into a σ-bond.

At this moment, V-V pairs of ions, called "dimers", are formed. The formation of dimers distorts the crystal lattice lowering its symmetry from tetragonal to monoclinic. The convergence of vanadium atoms means that the distance between vanadium ions inside a pair (or, in other words, a dimer) is less than the distance between the pairs. Therefore, the period of the crystal lattice along the one-dimensional chain of dimers during the formation of V-V pairs doubles. As a result of this structural transition from the metallic phase at $T > T_c$ to the semiconducting phase at $T < T_c$, called the Peierls transition, a gap in the electronic spectrum is formed. In this case, the $3d||$-band of the metallic phase splits into two Hubbard subbands (Ilinskiy et al. 2012; Il'inskiy et al. 2017), each of which contains half the number of levels of the original $d||$-band.

The lower subband turns out to be almost completely filled with electrons, according to the Pauli principle, while the upper one remains empty (up to the thermal transfer of electrons through the energy gap). Due to the formation of a gap in the energy spectrum, the VO_2 crystal becomes a semiconductor. According to the experiment, the width of the forbidden zone of the semiconductor is 0.7 eV. Hence, it follows that VO_2 in the proposed model should remain a semiconductor at temperatures for which the energy $K_BT = 34\ meV$ (at T = 340 K) cannot populate the conduction band through the *700 meV* gap. At the same time, the experiment says that VO_2 at T > 340K becomes a metal.

The model requires elaboration.

There is no doubt about the formation of dimers at T < 340 K, since numerous experimental data (X-ray structural analysis, EPR and NMR studies, Raman spectroscopy, etc.) confirm the formation

 https://www.doi.org/10.33910/2687-153X-2022-3-1-43-50

of dimers with a decrease in the lattice symmetry from tetragonal to monoclinic at $T < T_c$. But even a complicated model of a nonrigid quasi-one-dimensional chain, in which V-V dimers can appear and disappear, cannot explain the fact of thermal SMPT. Indeed, an increase in temperature to the critical value T_c = 340 K at a gap of *0.7 eV* (k_BT = *34 meV)* between the filled lower *3d* subband and the empty conduction band cannot lead to thermal destruction of the critical number of dimers required for the metallisation of the sample. That is, with the help of an energy of *30–40 meV* bring through the gap of *700 meV* the number of electrons that is needed to destroy the dimers is impossible. Therefore, the described model requires further elaboration.

At this stage of the construction of a complicated (SMPT) model, it is reasonable to use the well-known consideration of Mott (Mott 1997) regarding the problem of the behavior of an electron in the field of a one-dimensional chain. Such consideration is insufficient for a description in case of one-partial approximation. It is necessary to take into account the many-partial interaction, that is, the interaction between the electrons in the periodic field of the lattice. The effects caused by such interaction are defined by the term "correlation effects", and the correction to the energy of the bands caused by them is defined as the correlation energy (Gatti et al. 2007).

To conclude, it should be noted that the correlation effects in vanadium dioxide are a consequence of the special properties of the atom V, which has an unfinished *3d* shell (No. 23 of the periodic table of elements). A fundamental property of the V atom is the strong dependence of the position of its energy levels on the population of electrons. As a result, the population of the 4S shell with electrons lowers its energy so much that it turns out to be below the 3d shell in energy. Vanadium oxides inherit the fundamental property of this element and obtain the dependence of the energy position of the energy bands on their population. This can be seen when analysing the electronic configurations of the elements K, Ca, Sc, Ti, V, and Cr located sequentially in the periodic table of elements. So, when analysing the electronic configuration K (element no. 19 with the $3d^04s^1$ configuration), a "strangeness" is found: it has the overlying *4s* shell filled, while the underlying *3d* shell remains empty. That is, the *4s* shell, having received an electron, is located lower than the *3d* shell in terms of energy. Only after saturation of the *4s* shell with electrons does the *3d* shell gets filled, starting from the Sc element (21: $3d^14s^2$) to the V element (23: $3d^34s^2$). Ongoing from V to the element Cr (24: $3d^54s^1$), the filling sequence is again violated. An additional Cr electron with respect to V, filling the *3d* level, lowers its energy and initiates the transition of an electron from the *4s* level to the *3d* level.

The reason for the decrease in energy is strong electron-electron interactions (electron-electron correlations) along with the interactions of electrons with the atomic nucleus. As a consequence, the positions of the atomic levels strongly depend on their population. This dependence is transferred to vanadium compounds, in particular, vanadium dioxide. Due to the correlation effects, the energy position of the VO_2 bands depends on their electron population. This dependence is such that an increase in the population lowers the energy of the bands, and the emptying of the bands enhances their energy. Therefore, a thermal (or optical) increase in the population of the energy bands located above the Fermi level leads to a decrease in their energy, that is, to a decrease in the band gap E_g. This leads to structural SMPT in VO_2 at a relatively low temperature T = 340 K.

Conclusions

The Mott-Peierls SMPT in crystalline VO_2 films is determined, in addition to what is described above, by the martensitic nature of this phase transformation. As the temperature increases, the structural SMPT at the critical temperature $T = T_{cII}+\Delta T_{II}$ (ΔT_{II}—the half-width of the elementary hysteresis loop of the nanocrystallite) first targets "small" grains of the film despite their relatively wide elementary hysteresis loop. Following SMPT in "small" grains, structural SMPT occurs in "large" grains at $T = T_{cI}+\Delta T_I$.

This sequence is due to the fact that the phase equilibrium temperature T_{cII} of "small" grains, corresponding to the middle of the elementary loop, is significantly lower than T_{cI} of "large" grains. The reason is the technology behind the synthesis of nanocrystalline VO_2 films.

Thus, it can be stated that the separation of nanocrystallites of the film during its synthesis into two sets—"large" and "small"—is what makes the described SMPT mechanism in VO_2 films special. In this case, "small" nanocrystallites have a higher concentration of free electrons due to the presence of oxygen vacancies arising during the film synthesis. As a result, they have a smaller band gap (due to the correlation effects) and a smaller value of T_{cII}. The role of nanocrystallites of various sizes in SMPT in VO_2 films has been repeatedly discussed earlier. However, our work is the first to experimentally separate the

contributions of "large" and "small" nanocrystallites to SMPT and show that these contributions really differ greatly in the value of critical temperatures. The new experimental data were possible to obtain by dielectric spectroscopy. It turned out that dielectric spectroscopy is capable of separate identification of the electrophysical parameters of various sets of nanocrystallites randomly mixed on the surface of the VO_2 film.

To provide evidence, our article considers a simple case in which dielectric spectroscopy makes it possible to separately study nanocrystallites of different sizes. The size distribution of nanocrystallites can also be recorded using an electron or atomic force microscope (Fig. 1). However, nanocrystallites can be approximately the same size, but have different electrical properties. For example, nanocrystallites doped with different impurities or having different concentrations of the same impurity are not likely to be distinguished by microscopic methods. Dielectric spectroscopy, in this case, turns out to be a very convenient research tool. The nontrivial results of such more complex research options are described in detail in (Ilinskiy et al. 2020).

Conflict of interest

The authors declare that they have no conflicts of interest.

References

Castro, R. A., Ilinskij, A. V., Pashkevich, M. E. et al. (2021) *Dielektricheskaya spektroskopiya soedinenij sil'nokorrelirovannykh elementov [Dielectric spectroscopy of compounds of strongly correlated elements]*. Saint Petersburg: Fora-print Publ., 54 p. (In Russian)

Gatti, M., Bruneval, F., Olevano, V., Reining, L. (2007) Understanding correlations in vanadium dioxide from first principles. *Physical Review Letters*, 99 (26), article 266402. https://www.doi.org/10.1103/PhysRevLett.99.266402 (In English)

Il'inskiy, A. V., Pashkevich, M. E., Shadrin, E. B. (2017) Stage-by-stage modeling of the mechanism of semiconductor–metal phase transition in vanadium dioxide. *St. Petersburg Polytechnical University Journal: Physics and Mathematics*, 3 (3), 181–186. https://doi.org/10.1016/j.spjpm.2017.09.002 (In English)

Ilinskiy, A. V., Kastro, R. A., Pashkevich, M. E., Shadrin, E. B. (2020) Dielectric spectroscopy and mechanism of the semiconductor–metal phase transition in doped VO_2:Ge and VO_2:Mg Films. *Semiconductors*, 54 (4), 403–411. https://doi.org/10.1134/S1063782620040077 (In English)

Ilinskiy, A. V., Kvashenkina, O. E., Shadrin, E. B. (2012) Nature of the electronic component of the thermal phase transition in VO_2 films. *Semiconductors*, 46 (9), 1171–1185. https://doi.org/10.1134/S1063782612090096 (In English)

Mott, N. F. (1997) *Metal-insulator transitions*. London: Taylor and Francis Publ., p. 286. (In English)

Prokhorov, A. M. (ed.). (1994) *Fizicheskaya entsiklopediya. T. 4: Pojntinga — Robertsona strimery [Physical encyclopedia. Vol. 4: Pointing—Robertson streamers]*. Moscow: Bol'shaya Rossijskaya entsiklopediya Publ., 704 p. (In Russian)

Shadrin, E. B., Il'inskii, A. V. (2000) On the nature of metal–semiconductor phase transition in vanadium dioxide. *Physics of the Solid State*, 42 (6), 1126–1133. https://doi.org/10.1134/1.1131328 (In English)